A Joint Inversion-Segmentation approach to Assisted Seismic Interpretation

M. Ravasi, C. Birnie

Abstract

Structural seismic interpretation and quantitative characterisation are intertwined processes, which benefit from each others' intermediate results. In this work, we redefine them as an inverse problem that tries to jointly estimate subsurface properties (e.g., acoustic impedance) and a piece-wise segmented representation of the subsurface based on user-defined *macro-classes*. By inverting for these quantities simultaneously, the inversion is primed with prior knowledge about the regions of interest, whilst at the same time it constrains this belief with the actual seismic measurements. As the proposed functional is separable in the two quantities, these are optimized in an alternating fashion, and each sub-problem is solved using a Primal-Dual algorithm. Subsequently, an ad-hoc workflow is proposed to extract the perimeters of the detected shapes in the different segmentation classes and combine them into unique seismic horizons. The effectiveness of the proposed methodology is illustrated through numerical examples on both synthetic and field datasets.

A Joint Inversion-Segmentation approach to Assisted Seismic Interpretation

Introduction

Seismic interpretation represents an important step in the mapping and characterisation of subsurface structures and is traditionally composed of two parts: structural and quantitative interpretation. The former aims at identifying the geological framework (i.e., horizons and faults) whilst the latter focuses on retrieving subsurface properties. Historically, structural interpretation is mainly carried out manually and led by geological understanding, whilst post- and pre-stack inversion represent the workhorses in the process of quantitative characterisation of the subsurface. Despite the fact that structural information can undoubtedly provide valuable prior knowledge to the property estimation process and elastic properties can aid structural interpretation, these two processes are traditionally performed independently from each other in a sequential fashion.

In this work, we propose a computer-aided seismic interpretation framework based on the solution of a joint inversion-segmentation optimisation problem. The input is limited to post-stack seismic data and the definition of a number of acoustic classes as identified from available well logs. Examples on synthetic and field datasets show that our methodology can successfully recover key structures as defined by the interpreter in a fully automatic manner. Moreover, as a by-product of our algorithm, both an acoustic impedance (AI) and a segmentation model are retrieved that can be used as inputs to subsequent steps of reservoir modelling.

Joint Inversion-Segmentation

Inspired by the work of Corona et al. (2019) on joint reconstruction and segmentation in the context of medical imaging, we define a functional to jointly invert seismic data for their acoustic impedance as well as a segmented representation of the subsurface composed of N_c classes, each of which is characterised by a different range of AI values. The functional for our specific problem can be written as:

$$(\mathbf{m},\mathbf{V}) = \underset{\mathbf{m},\mathbf{V}\in C}{\operatorname{argmin}} \quad \frac{1}{2}||\mathbf{d}-\mathbf{G}\mathbf{m}||_2^2 + \alpha TV(\mathbf{m}) + \delta \sum_{j=1}^{N_c}\sum_{i=1}^{N_xN_z} V_{ji}(m_i - c_j)^2 + \beta \sum_{j=1}^{N_c} TV(\mathbf{V}_j^T) \qquad (1)$$

where $\mathbf{m}$ is a vector of size $N_xN_z \times 1$ that contains the natural logarithm of the acoustic impedance model and $\mathbf{c}$ is a vector of size $N_c \times 1$ which contains the acoustic impedance values associated to each class. $\mathbf{G} = \mathbf{W}\mathbf{D}$ is the post-stack modelling operator composed of a first derivative operator $\mathbf{D}$ and a convolutional operator $\mathbf{W}$ whose convolution kernel is the estimated wavelet w divided by 2, and $\mathbf{d}$ is post-stack seismic data of size $N_xN_z \times 1$. Here, we use the convention that x_i is the i-th element of a vector and $\mathbf{X}_i$ represents the extraction of the i-th column of a matrix (whilst $\mathbf{X}_j^T$ is the j-th row of a matrix transposed into a column vector). $\mathbf{V}$ is a matrix of size $N_c \times N_xN_z$, where each column is constrained to be in the unit Simplex, $C = \{(\mathbf{V}_i \in \mathbb{R}^+ : V_{ji} \geq 0, \sum_{j=1}^{N_c} V_{ji} = 1\} \quad \forall i = 1,2,...,N_zN_x$. Note that by ensuring the sum of the elements of each column of $\mathbf{V}$ to be equal to 1 and every element to be positive, we can interpret such values as the probability of each point in the subsurface belonging to a certain class. The Total Variation (TV) regularisation term is defined as $TV(\mathbf{x}) = ||\nabla\mathbf{x}||_{2,1} = \sum_{i=1}^{N_xN_z}\sqrt{(\mathbf{x}_x)_i^2 + (\mathbf{x}_z)_i^2}$ where $\nabla : \mathbb{R}^{N_xN_z} \rightarrow \mathbb{R}^{2\times N_xN_z}$ is the gradient operator that transforms a vector into a matrix whose rows contain the derivatives $(\mathbf{x}_x)$ and $(\mathbf{x}_z)$ computed along the x- and z directions, respectively. Finally, α, β, and δ are regularisation parameters used to balance the inversion and segmentation terms of the functional.

The functional in equation 1 is non-convex in the joint argument $(\mathbf{m},\mathbf{V})$, however it is convex in each individual variable space. A splitting approach is therefore used to minimise two convex problems in an alternating fashion. Moreover, since solving TV-regularised problems can lead to a systematic loss of contrast in the estimated model, both TV regularisation terms are replaced by their generalised Bregman distance ($D_{TV}^{\mathbf{p}}(\mathbf{u},\mathbf{u}') = TV(\mathbf{u}) - TV(\mathbf{u}') - (\mathbf{u}-\mathbf{u}')^T\mathbf{p}$) and Bregman iterations are introduced to solve each independent minimisation problem. The overall algorithm reads as:

$$\mathbf{m}^k = \underset{\mathbf{m}}{\text{argmin}} \quad \frac{1}{2}||\mathbf{d}-\mathbf{G}\mathbf{m}||_2^2 + \alpha(TV(\mathbf{m}) - \mathbf{m}^T\mathbf{p}^{k-1}) + \delta\sum_{j=1}^{N_c}\sum_{i=1}^{N_xN_z} V_{ji}^{k-1}(m_i - c_j)^2 \tag{2a}$$

$$\mathbf{p}^k = \mathbf{p}^{k-1} - \frac{1}{\alpha}\left(\mathbf{G}^T(\mathbf{G}\mathbf{m}^k - \mathbf{d}) + 2\delta\sum_{j=1}^{N_c}\mathbf{V}_j^T\cdot(\mathbf{m}^k - c_j)\right) \tag{2b}$$

$$\mathbf{V}^k = \underset{\mathbf{V}\in C}{\text{argmin}} \quad \delta\sum_{j=1}^{N_c}\sum_{i=1}^{N_xN_z} V_{ji}(m_i^k - c_j)^2 + \beta\sum_{j=1}^{N_c}(TV(\mathbf{V}_j^T) - (\mathbf{V}_j^T)^T\mathbf{Q}_j^{T\,k-1}) \tag{2c}$$

$$Q_{ji}^k = Q_{ji}^{k-1} - \frac{\delta}{\beta}(m_i^k - c_j)^2 \quad \forall i,j \tag{2d}$$

where $\mathbf{p}$ and $\mathbf{Q}$ are the sub-gradients of their corresponding Bregman distances and $\cdot$ indicates element-wise multiplication. Equations 2a and 2c are solved using the Primal-Dual (PD) algorithm of Chambolle and Pock (2011), a solver in the family of proximal algorithms that is able to minimize non-smooth, convex functionals of the form, $\hat{\mathbf{x}} = \underset{\mathbf{x}}{\text{argmin}}\, f(\mathbf{K}\mathbf{x}) + \sum_i \mathbf{x}^T\mathbf{z}_i + g(\mathbf{x})$, provided that the proximal operators of the f and g functions can be computed (Parikh, 2013). Whilst other proximal solvers have been used to include TV-regularizion in post- and pre-stack seismic inversion (Gholami, 2015; Kolbjornsen et al., 2019), the PD solver possesses higher flexibility and the possibility to handle additional terms in the form of dot products (e.g., $\mathbf{m}^T\mathbf{p}^{k-1}$ term in our equation 2a). To recast equation 2a in the form required by the PD solver, we write $\mathbf{K} = \nabla$, $\mathbf{z} = -\alpha\mathbf{p}^{k-1}$, $f = ||\,||_{2,1}$, and $g = \frac{1}{2}||\hat{\mathbf{d}} - \hat{\mathbf{G}}\mathbf{m}||_2^2$ with:

$$\hat{\mathbf{G}} = \begin{bmatrix}\mathbf{G}\\ \sqrt{2\delta}\hat{\mathbf{V}}\end{bmatrix},\ \hat{\mathbf{d}} = \begin{bmatrix}\mathbf{d}\\ \sqrt{2\delta}\hat{\mathbf{c}}\end{bmatrix},\ \hat{\mathbf{V}} = \begin{bmatrix}diag\{\sqrt{\mathbf{V}_1^T}\}\\ \dots\\ diag\{\sqrt{\mathbf{V}_{N_c}^T}\}\end{bmatrix},\ \hat{\mathbf{c}} = \begin{bmatrix}\sqrt{\mathbf{V}_1^T}c_0\\ \dots\\ \sqrt{\mathbf{V}_{N_c}^T}c_{N_c}\end{bmatrix} \tag{3}$$

where the proximal operators of g can be obtained by approximately solving the least-squares functional and that of f is the well-known proximal of the isotropic TV norm. Equation 2c can be written as:

$$\mathbf{v}^k = \underset{\mathbf{v}\in C}{\text{argmin}} \quad \mathbf{v}^T(\delta\mathbf{g} - \beta\mathbf{q}^{k-1}) + \beta\sum_{j=1}^{N_c} TV(\mathbf{V}_j^T) \tag{4}$$

where $\mathbf{v} = Vec(\mathbf{V})$ and $\mathbf{q} = Vec(\mathbf{Q})$ are the vectorised version of $\mathbf{V}$ and $\mathbf{Q}$, respectively. Moreover, $\mathbf{g} = ((\mathbf{m}-c_0)^2, .., (\mathbf{m}-c_{N_c})^2)^T$ is defined as the weighting vector, where the superscript 2 is used to indicate the squared difference between each element of the vector $\mathbf{m}$ and the chosen coefficient c_j. By writing $\mathbf{K} = \nabla$, $\mathbf{z} = \delta\mathbf{g} - \beta\mathbf{q}^{k-1}$, $f = ||\,||_{2,1}$, and $g = i_C$ (i.e., the indicator of the Simplex function), equation 4 is also shown to be in the form required by the PD solver. The algorithm described in equation 2 is implemented here using the PyLops framework (Ravasi and Vasconcelos, 2020).

Horizon Extraction

In order to extract horizons from the outcome of the segmentation step, each class probability is first binarised with a threshold equal to $th = 0.5$. TV-norm is then used to enhance the edges of the binarised bodies. These are further selected as a list of possible horizon points and joined in a left-right marching fashion to create horizon lines, which are subsequently labeled based on the most likely class appearing above and/or below each line. After repeating the above procedure for all classes, horizon lines with the same label are joined based on a distancing threshold to create the final horizons.

Synthetic example

The synthetic example is based on a modified version of the SEG Hess VTI model (Fig.1a). Data are modelled using an 8Hz Ricker wavelet to which spatially coloured noise is added (Fig.2b). We assume knowledge of the different zones in the model and their corresponding AI value to define the

class vector **c**. Fig.1b shows the estimated model for a spatially regularised least-squares inversion, whilst the model produced after 3 iterations of our joint inversion-segmentation algorithm is displayed in Fig.1c. The inversion process benefits from the use of the TV-norm which acts as a better regulariser when compared to the L2-norm of spatial derivatives; ultimately, the estimated model presents sharp discontinuities and less imprint from the noise in the data. Least-squares inversion also underestimates the acoustic impedance of the salt body; this is because the frequency content of the seismic data does not allow to recover such a frequency gap unless facilitated by the use of a stronger prior. The retrieved model from our algorithm instead more closely resembles the true model, especially for the salt body whose absolute value is more accurately estimated. Such improvements are the direct consequence of the TV regularisation term as well as the fact that the first step of segmentation is used as a soft constraint to the second step of inversion, whose output is in turn used to drive the second step of segmentation. The outcome of the last segmentation step (Fig.2c) is of much higher quality compared to performing segmentation after least-squares inversion (Fig.2a). The tracked horizons are also of overall higher quality especially on the left side of the salt body and in the deeper part of the model (Fig.2b and d).

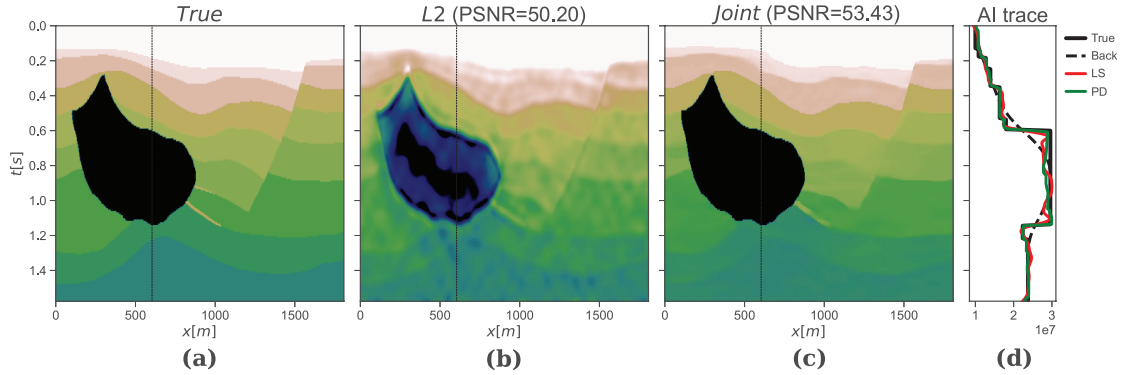

Figure 1 *a) True Hess acoustic impedance model. b) Least-squares inversion and c) Joint inversion-segmentation model estimates. d) AI traces along well trajectory for different models.*

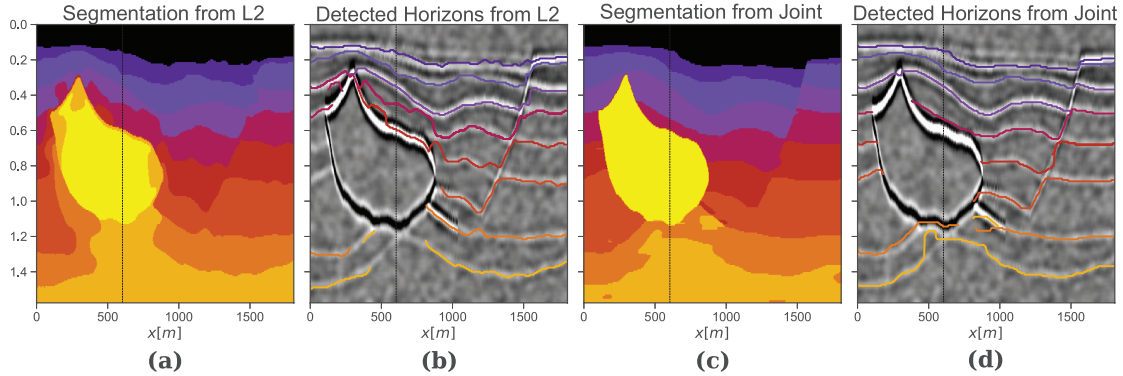

Figure 2 *a,c) Segmented model from L2 and Joint inversion, respectively. b,d) Tracked horizons from L2 and Joint inversion, respectively, overlaid on the input seismic data.*

Field data example

In this section, our joint inversion and segmentation algorithm is applied to a time migration section of the Volve dataset passing through the NO/15-9 19 BT2 well (Fig.3e). The manually interpreted horizons (Top Ty in green, Top Shetland in blue, and BCU in yellow) are overlaid on the seismic section and their corresponding well markers are shown in Fig.3b alongside the acoustic impedance log, which is used to define 4 different classes ($\mathbf{c} = [4000, 7600, 10200, 13000]$) as input to the segmentation algorithm. A background model is built from the root-mean-square velocity model, which is first converted into interval velocities and subsequently calibrated with the acoustic impedance log. The estimated AI

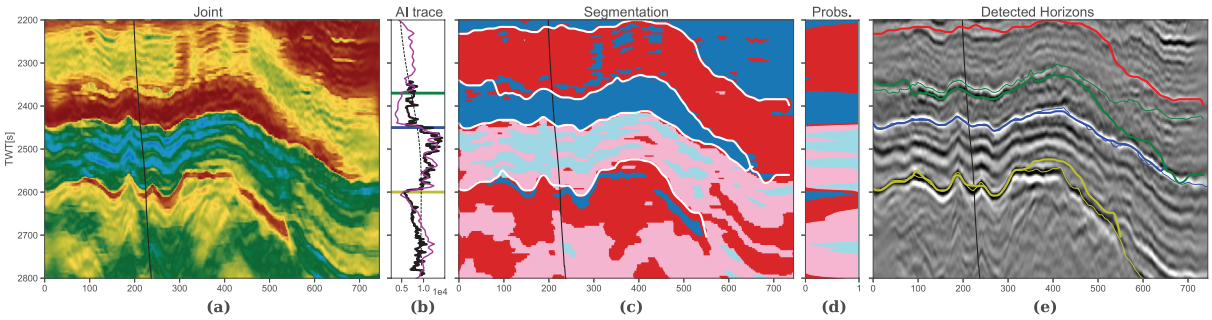

Figure 3 *a) Inverted AI model and b) AI profiles along well trajectory (solid: log, dashed: background, purple: inverted). c) Segmented model with tracked horizons (white lines). d) Class probabilities along well. e) Input seismic data with tracked horizons (colored lines) and available horizons (thin lines).*

model for our inversion scheme is shown in Fig.3b. TV regularised inversion creates sharp transitions in the impedance values which are generally overpredicted (or underpredicted) by least-squares inversion due to the lack of low frequency information in the data. An overall good match is observed with the AI log along the well trajectory (Fig.3b). Fig.3c and d display the segmented model alongside the probabilities of each class along the well trajectory. White lines represent the horizons that have been extracted from the different class probabilities. The tracked horizons (thick lines) are also shown in Fig.3e alongside the manually interpreted horizons (thin lines). The Top Shetland formation is successfully tracked and the resulting horizon is very similar to the manually interpreted one. On the other hand, our interpretation of Top Ty diverges from the manual interpretation towards the right side of the model; a similar behaviour is also observed for the horizon above. By looking at the inverted AI model in Fig.3a, we observe a thinning of the Ty formation that is consistent with the tracked horizons. Whilst the quality of the seismic data prevents us to determine if our interpreted horizons are correct, this result highlights the direct connection between the tracking and inversion steps. Finally, our algorithm is able to track part of the BCU horizon, failing to do so when the thin, low AI layer is eroded out on the right side of the model. Overall, these results confirm the validity of our algorithm and its usefulness in jointly solving a number of tasks in the seismic interpretation process whilst keeping consistency among the results.

Conclusions

We have presented a new approach to assisted seismic interpretation which provides not only a set of interpreted horizons but also both a property model and a segmented model of the subsurface. Acoustic properties are not only inverted for from seismic data, but they are also used as input to define a direct link between well log responses and the expected horizons to be extracted in the final step of our workflow. Our work also remarks on the importance of enforcing blockiness in the inversion of seismic data, which is obtained here via a combination of regularisation (Total Variation), solver (Primal-Dual) and additional constraints (the segmentation term). Sharper models help the segmentation step and may also have wider implications when used as hard or soft constraints in facies or property modelling. The extension of our algorithm to pre-stack and waveform inversion is the subject of ongoing research.

References

[1] Chambolle, A., and Pock, T. [2011] A first-order primal-dual algorithm for convex problems with applications to imaging. Journal of Mathematical Imaging and Vision.

[2] Corona, V., Benning, M., et al. [2019] Enhancing joint reconstruction and segmentation with non-convex Bregman iteration. Inverse Problems.

[3] Gholami, A. [2015] Nonlinear multichannel impedance inversion by total-variation regularization. Geophysics.

[4] Ravasi, M., and Vasconcelos, I. [2011] PyLops—A linear-operator Python library for scalable algebra and optimization. SoftwareX.

[5] Kolbjornsen, O., Evensen, O., Nilsen, A. K., and Lie, J. E. [2019] Digital superresolution in seismic AVO inversion. The Leading Edge.

[6] Parikh, N. [2013] Proximal Algorithms. Foundations and Trends in Optimization.